IOP Publishing Quantum Sci. Technol. 8 (2023) 044001 https://doi.org/10.1088/2058-9565/ace1a3

Quantum Science and Technology

OPEN ACCESS

RECEIVED
5 September 2022

REVISED
28 February 2023

ACCEPTED FOR PUBLICATION
26 June 2023

PUBLISHED
10 August 2023

PAPER

Microgravity facilities for cold atom experiments

Matthias Raudonis[1,*], Albert Roura[1], Matthias Meister[1], Christoph Lotz[2], Ludger Overmeyer[2], Sven Herrmann[3], Andreas Gierse[3], Claus Lämmerzahl[3], Nicholas P Bigelow[4], Maike Lachmann[5], Baptist Piest[5], Naceur Gaaloul[5], Ernst M Rasel[5], Christian Schubert[6], Waldemar Herr[6], Christian Deppner[6], Holger Ahlers[6], Wolfgang Ertmer[6], Jason R Williams[7], Nathan Lundblad[8] and Lisa Wörner[1]

[1] German Aerospace Center (DLR), Institute of Quantum Technologies, Wilhelm-Runge-Straße 10, 89081 Ulm, Germany
[2] Institute of Transport and Automation Technology, Leibniz University Hannover, An der Universität 2, 30823 Garbsen, Germany
[3] Center of Applied Space Technology and Microgravity, University Bremen, Am Fallturm 2, 28359 Bremen, Germany
[4] Department of Physics and Astronomy, Institute of Optics, Center for Coherence and Quantum Optics, The University of Rochester, Rochester, NY 14627, United States of America
[5] Institute of Quantum Optics, Leibniz University Hannover, Welfengarten 1, 30167 Hannover, Germany
[6] German Aerospace Center (DLR), Institute for Satellite Geodesy and Inertial Sensing, c/o Leibniz University Hannover, DLR-SI, Callinstr. 36, 30167 Hannover, Germany
[7] Jet Propulsion Laboratory (JPL), 4800 Oak Grove Drive, Pasadena, CA 91109-8001, United States of America
[8] Bates College, Department of Physics and Astronomy Carnegie Science Hall, Room 322, Lewiston, ME 04240-6020, United States of America
[*] Author to whom any correspondence should be addressed.

E-mail: matthias.raudonis@dlr.de

Keywords: drop tower, free fall, sounding rocket, parabolic flight, atom interferometry, Bose–Einstein condensate, fundamental physics

Abstract

Microgravity platforms enable cold atom research beyond experiments in typical laboratories by removing restrictions due to the gravitational acceleration or compensation techniques. While research in space allows for undisturbed experimentation, technological readiness, availability and accessibility present challenges for experimental operation. In this work we focus on the main capabilities and unique features of ground-based microgravity facilities for cold atom research. A selection of current and future scientific opportunities and their high demands on the microgravity environment are presented, and some relevant ground-based facilities are discussed and compared. Specifically, we point out the applicable free fall times, repetition rates, stability and payload capabilities, as well as programmatic and operational aspects of these facilities. These are contrasted with the requirements of various cold atom experiments. Besides being an accelerator for technology development, ground-based microgravity facilities allow fundamental and applied research with the additional benefit of enabling hands-on access to the experiment for modifications and adjustments.

1. Introduction

Terrestrial gravitational pull affects experiments in ground-based laboratories. This has an impact on fundamental and applied research in various areas, ranging from life sciences [1–3], to studies of alloys [4, 5], propulsion [6, 7] and fundamental physics [8, 9]. For some of the research topics, countermeasures can be employed to act against gravity, enabling experimentation [10–12]. However, most of these measures present challenges, e.g. a detrimental distortion of the potentials acting on the studied subject. With those additional parasitic forces, experimentation on weak effects can be challenging or be rendered impossible.

Alternatively, the complete experimental apparatus can subjected to free fall, creating a situation in which the subject of study falls with the observing system, thus appearing stationary. While the gravitational pull still acts on such an experiment platform, this is often referred to as the 'microgravity environment', describing the acceleration of the object of study with respect to the detection systems.

A possibility for achieving a persistent microgravity environment is the operation on a space-borne platform. There, the experiment is constantly falling towards and around a body of gravity. This operation is

costly and restricted by many factors, such as technological maturity, miniaturization, power consumption, limited sample size, and automation.

Possibilities to achieve microgravity environments on Earth are based on dropping the experiment platform into free-fall, leading to microgravity of the experiment with respect to the apparatus. Several facilities have been developed, including worldwide efforts like the 2.2 s and 5.2 s NASA Glenn Research Center Drop Towers [13, 14], the 2.2 s Kingston Micro-Gravity Drop Tower [15], the 3.5 s Beijing Drop Tower [16] and the retired 10 s JAMIC Drop Tower [17]. Additional means, such as large atomic fountains [18–21], will not be covered in this paper, as those represent specific experiments as opposed to microgravity facilities for usage by multiple experiments.

In this paper we focus on the following facilities:

(i) Einstein-Elevator in Hannover, Germany
(ii) Drop tower in Bremen, Germany
(iii) GraviTower Prototype in Bremen, Germany
(iv) Parabolic flights from Bordeaux, France
(v) Sounding rockets launched from Kiruna, Sweden.

These facilities offer unique cold atom study opportunities to researchers as well as bridging the technology readiness gap for payloads and partly already supported cold atom experiments. Therefore, they will be individually described and their main capabilities best suitable for cold atom experiments discussed. The critical parameters as achievable microgravity conditions, repetition rates, microgravity durations and payload constraints will be discussed.

2. Cold and condensed atom experiments in microgravity

Microgravity provides multiple advantages for experiments on atom optics and interferometry. For an overview over different possibilities, see, for instance, [22]. This section is dedicated to provide a short overview over the benefit of microgravity conditions for cold atom experiments, individual ideas of which will be outlined in greater detail in section 5.

Degenerate quantum gases are trapped in optical and magnetic fields. Optical and magnetic fields enable trapping and suspending cold atoms and allow for a wide range of fundamental studies [23, 24]. However, additional traps can lead to a distortion of the atomic cloud and complicate the observation of small effects.

In a perfectly isolated microgravity environment, the atomic cloud remains stationary with respect to the experimental setup without relying on compensation techniques. Such systems enable the study of weak trapping potentials and observing atomic ensembles after long evolution times. This, in turn, may allow for very low temperatures [25] and large scale factors in atom interferometry [26–29]. Space-borne atom interferometers were proposed for testing the UFF [30, 31], Earth observation [32–34], dark matter and dark energy search, and cosmology [35] has been proposed. Those and other possible applications of quantum technologies in space are summarized in several publications, see [31, 36].

Other areas, that benefit from microgravity environments are the study of novel topologies, such as 3D bubble shells [37, 38], surface interactions and quantum reflections [39], phase separation [40], and atom mixtures [41].

The long lead times and high cost of space missions, and the very limited or non-existent access to the device call for more flexible ways to develop the required technology, experimental designs and methods and investigate the associated scientific questions. Experiments on terrestrial microgravity platforms serve as pathfinders in preparation for such missions on orbital platforms and beyond.

Cold and condensed atoms are currently being studied in terrestrial microgravity platforms at length. Two major milestones for cold atom research in microgravity are the first Bose–Einstein condensate [9] and the first atom interferometer [26] produced in microgravity. The experimental results stemming from the QUANTUS collaboration are expanded by the results of the I.C.E. collaboration [42] in parabolic flights, the PRIMUS collaboration [43] in drop tower experiments, and the first MAIUS campaign on a sounding rocket [44, 45].

The second generation BEC apparatus of the QUANTUS collaboration [46] reached the lowest reported expansion rate, resulting in an internal kinetic energy of $U_{\mathrm{kin}} = \frac{3}{2}k_{\mathrm{B}} \cdot 38\,\mathrm{pK}$ using a time-domain matter-wave lens system consisting of collective-mode excitation and delta-kick collimation that enables the BEC to be detected after tens of seconds [25]. This is a prerequisite for long atom interferometer times in microgravity. With those successful experiments the road towards more advanced studies of cold and condensed atoms in terrestrial and orbital microgravity platforms is paved.

3. Facilities

Certain classes of cold atom experiments benefit essentially from microgravity conditions, as previously described. Effects masked by gravity can thus be investigated. As previously described, microgravity can be generated on Earth by dropping the experiment. This requires constant acceleration equal to the local gravity parameter g. The microgravity time is thus generally limited by the falling distance s, as seen in equation (1). The facilities below all follow this principle by different means of engineering

$$\ddot{s} = g \qquad\qquad s = \frac{1}{2} g t^2.$$

Equation 1. Microgravity can be achieved with a constant acceleration equal to the gravitational acceleration g. The vertical displacement of the falling object s is calculated by the second integration over the free fall time t.

With terrestrial microgravity in different facilities, efficient possibilities for research on very small quantum physical effects, general research for space applications, and the development of space-qualified hardware are created. This section discusses selected ground-based facilities and their capabilities.

3.1. Einstein-Elevator

The Einstein-Elevator at Leibniz University Hannover is a young facility for research under different gravitational conditions [47]. The development was initiated in 2009 out of the former Cluster of Excellence QUEST and research operations began in October 2019. The development of a novel drop tower facility was started with the vision of being able to study the effects of quantum physics efficiently, cost effectively and with low expenditure of time. This was enabled by an advanced automated facility concept. Besides the focus on quantum optical experiments with projects like DESIRE [48–50], other research-relevant topics in the field of mechanical engineering have emerged in the last years. These topics also brought up a new research area at Leibniz University Hannover/ITA, dealing with production technologies under space conditions [51–53]. The current research in the Einstein-Elevator is divided by four major topics: fundamental physics research with focus on quantum optical experiments, production technologies under space conditions, facility enhancements with expanding the research possibilities as well as increasing the quality of the system and service operations to make the facility available to national and international researchers [54].

The Einstein-Elevator is a third generation drop tower (first: pure vacuum tubes/shafts, second: vacuum tube/shaft with catapult, third: direct driven small vacuum chamber) and the first system to go into operation. The 40 m facility with a drop height of 20 m is offering 4 s of microgravity. As an extension to classic drop towers, it features a novel guidance and drive concept [47, 55, 56]. A linear drive accelerates a gondola (vacuum chamber) with an integrated experimental setup. It provides the necessary acceleration, realizes the control of the precisely previously calculated motion and also compensates for any rolling and air resistance that occurs during the fast movement of the gondola inside the building. This opens up a number of new opportunities that are urgently needed by the scientific community. Statistical studies can be carried out with a repetition rate of 300 experimental runs per day in a three shift operation. In addition, the drives mounted along the travel path make it possible for the first time for an Earth-based facility to simulate not only weightlessness but also other partial gravitational environments like Lunar or Martian gravity. The large dimensions and high mass of an experiment also allow more elaborate setups. It also reduces the necessary effort to miniaturize an existing experimental laboratory setup. The experiments may be 1.7 m in diameter and 2.0 m in height and weight up to 1000 kg including the experiment carrier. An effective payload of about 550 kg (up to 770 kg for vacuum compatible experimental setups) is available.

The experiment carrier is located in a vacuum atmosphere (10^{-2} mbar) for acoustic decoupling during free fall. Due to the frequent requirement of not wanting/being able to design the experiment hardware to be suitable for vacuum and to accommodate it in a normal atmosphere, the experiment carrier consists of an optional, pressure-tight shell, the experiment support structure and the carrier base. A wide range of equipment is available in the experiment carrier. An onboard computer records accelerations, rotations, magnetic fields, temperatures, pressures, humidity and various other signals. In addition high-speed cameras and surveillance cameras tested for this application can be used to observe the experiments. The telemetry and experiment data is transmitted continuously, even during the flight phase, using optical transceivers. A power supply (permanent 24 V, 16 A, in parking level also 230 V and customized power supplies), a vent line for vacuum pumps and a cooling water system with up to 1 kW are also available.

Figure 1. Start position of the Einstein-Elevator gondola for a vertical parabolic flight (credit: Leibniz University Hannover/Marie-Luise Kolb, licence: CC-BY 3.0 DE).

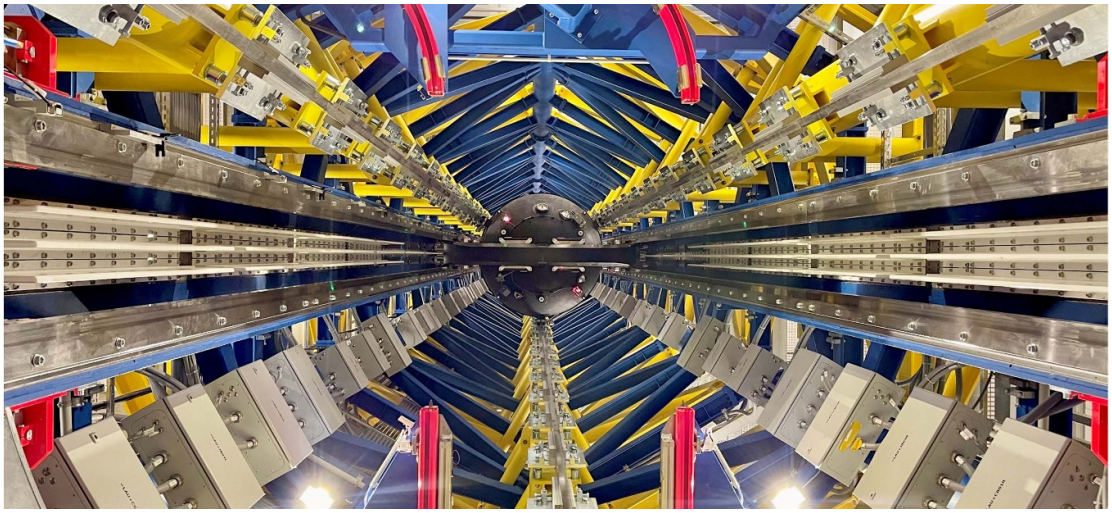

Figure 2. Movement of the Einstein-Elevator during a vertical parabolic flight (credit: Leibniz University Hannover/Christoph Lotz, licence: CC-BY 3.0 DE).

The experimental procedure includes the following steps:

(i) Integration of the experiment setup into the supporting structure of the experiment carrier.
(ii) Delivery of the fully assembled experiment to HITec.
(iii) Integration of the support structure into the carrier system and safety checks.
(iv) Insertion of the carrier into the gondola.
(v) Preparation for the launch by closing the gondola and evacuating the interior space.
(vi) Launch from lower position (4 s in μg, see figure 1) or upper position (2 s in μg).
(vii) Vertical parabolic flight or drop (see figure 2).
(viii) Safe deceleration.
(ix) Measurement data transfer.
(x) Preparing the next launch (continue at (vi)) or making some experiment adjustments (continue with (v)).

During launch, the 2700 kg of drive cart, traverse, and the gondola including the experiment are accelerated at 5 g by the 4.8 MW linear drive. A velocity of 20 m s^{-1} is achieved over the first 5 m. In contrast to classical drop tower systems, a release and catching mechanism is not required. The carrier stands unconnected on the bottom of the gondola and simply lifts off the ground shortly after reaching the final speed. Due to the controlled movement of the gondola and a balanced carrier, no horizontal movements occur that would cause the carrier to bump against the gondola walls. The distance between the gondola floor and the base of the experiment carrier is controlled to a defined distance of currently 50 mm during the complete flight phase. After the 20 m long upward and downward motion, the distance is reduced to zero again in a short time. The movement ends at the starting level after a joint deceleration of gondola and experiment. In addition to the catapult-like acceleration from the lower start position, it is also possible to start from the upper position if the experiment setup does not survive the 5 g of start acceleration or if just the transition from 1 to 0 g is to be simulated. At the end of the free fall, however, the same deceleration forces occur during braking as in the catapult-like mode. In this case the free-fall duration is reduced to half the time (2 s).

With the establishment of this direct driven/third generation facility, the following visions become achievable:

- Explore quantum effects with high statistical quality. Develop new technologies. Rapidly implement engineering demonstrations of these technologies at low cost to underpin larger missions.
- Establish new research fields such as research and development on production processes under space conditions. Enabling building spare parts in space or habitats on other planets.
- Make research under space conditions available to the broader research community through efficient, cost-effective, and rapid experimentation.

Novel drop towers such as the Einstein-Elevator enable the scientific community to gain tremendous advantages in the execution of their experiments: Time in microgravity by using drop towers is generally limited to a few seconds compared to parabolic flights, research rockets, or experiments on the ISS. But its availability/accessibility, repetition rate, microgravity-quality, payload mass, and volumes open new research opportunities, including for early experiment stages with low technology readiness level (TRL).

3.2. Drop tower

The Bremen drop tower has been operating continuously since 1990 and serves as a platform for stand-alone microgravity research but also for verification and testing of key components and mechanisms in payloads or hardware for satellites and other orbital platforms. Examples are the QUANTUS project with the first creation of a Bose–Einstein condensate in microgravity, the first BEC interferometry in microgravity and the use of delta-kick collimation in that context [9, 25, 26], verification of the T-SAGE accelerometer of the MICROSCOPE mission [57] or verification of the asteroid impact sampling device of the Hayabusa-2 space probe [58].

The tower stands at a total height of 146 m with an internal drop tube, which is decoupled from the outside structure and measures 122 m in height and 3.5 m in diameter (see figure 3). The available free fall time per drop is 4.7 s. At the bottom of the tube the experiment capsules are captured and decelerated inside a container filled with styrofoam pellets. This exposes the experiment to an average deceleration of 25 g in 200 ms with a peak just below 50 g. In order to eliminate air friction during free fall and reduce residual accelerations to a level of few parts of 10^{-6} g, the drop tube is evacuated to 0.1 mbar in about 90 min prior to the drop. After each drop, the tube is vented again for about 30 min to allow for recovery of the experiment. This procedure allows for typically three successive drops per day.

Typical experiment campaigns extend over days or weeks, with each experiment being integrated inside a drop capsule prior to a campaign, with assistance from the drop tower engineering team. In standard configuration the drop capsules allow for 500 kg total mass, which leaves ca. 264 kg for the payload at a maximum payload height of 1.7 m and 0.6 m in diameter. In drop mode the limitation on height and mass is not a strict limit and customized capsules with payloads exceeding 2.0 m with or to 680 kg have been operated as well. The standard configuration of the capsules is to provide an on-board computer for collecting house keeping data, a battery platform with 24 Ah and an interface for electrical connections to buffer the battery platform (24 V, 10 A) as well as for cooling media, allowing for 2.6 kW of cooling power.

Since 2004, the drop tower also incorporates a catapult system, that allows to extend the free fall time up to 9.3 s. This facility can launch catapult capsules of up to 400 kg (161 kg payload) and 0.95 m payload height. The catapult uses a combination of pneumatics and hydraulics to accelerate the experiment capsule placed on a piston at 18 g in about 280 ms (peak acceleration is 30 g). The combination of 9.3 s of free fall at

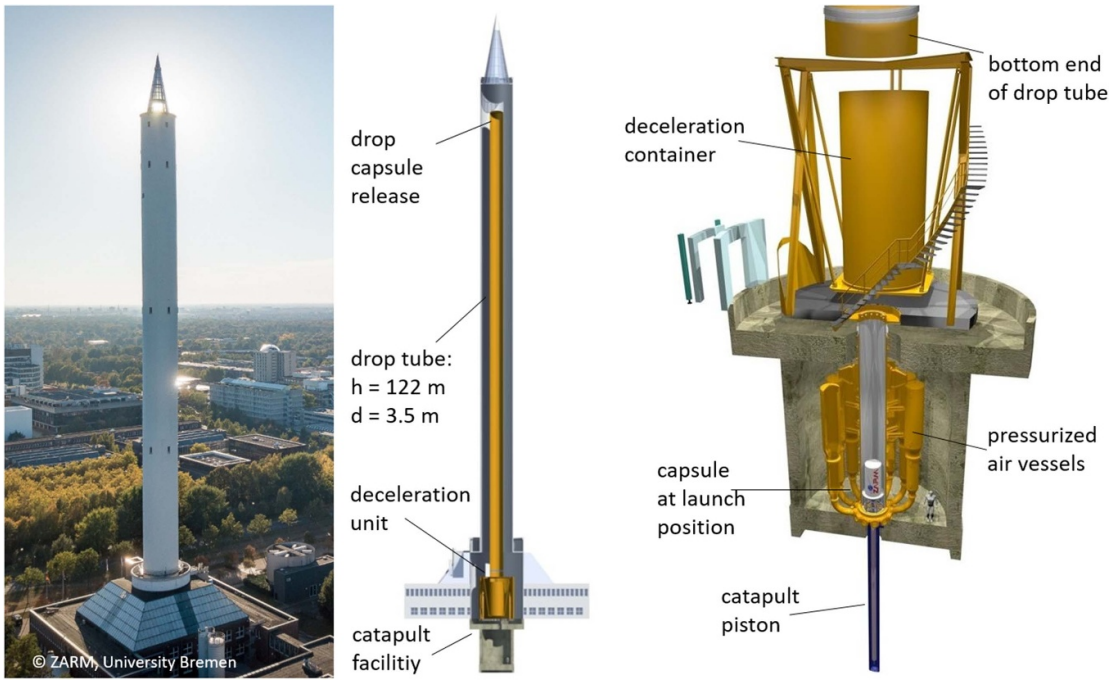

Figure 3. The drop tower at ZARM, University Bremen with a total height of 146 m, outside view and details of the deceleration unit and catapult system.

microgravity levels with low cost and easy accessibility is a unique feature of this facility. This allowed the consecutive creation of four BECs in one drop [59].

3.3. GraviTower prototype

The GraviTower Prototype is a scalable technology carrier for a big second drop tower currently in design (GraviTower) and also functions as a scientifically fully usable second drop tower at ZARM. The GraviTower Prototype offers 2.5 s of microgravity for experiments in the exact same experiment carriers as in the Bremen drop tower. Both platforms are fully compatible, so existing experiments do not have to be redesigned or adjusted to be operated in the GraviTower Prototype.

Figure 4 shows on the left side the tower/guiding system of the GraviTower Prototype with its doors open so you can see the slider with the ZARM logo on it. In the center the slider is shown with its doors open giving easy access to the experiment. On the right side the top part of the Release-Caging-Mechanism (RCM) is shown. This part of the RCM decouples all but the vertical translational degree of freedom during acceleration and also during microgravity.

The decision to build a 2.5 s prototype is driven by the demands of the PRIMUS and QUANTUS experiments to offer those research groups the desired high repetition rate. A high repetition rate is achieved by avoiding a vacuum chamber as used in drop towers and replacing it by an actively accelerated and rail guided drag shield, comparable with the Einstein-Elevator in section 3.1. The installed power of 3.5 MW of the drives allows to accelerate the experiment inside the drag shield with up to 5 g (or less if required by the experiment). A smooth harmonic time function can be chosen for the initial acceleration to minimize residual structural vibrations in the beginning of the microgravity time. During the initial acceleration or reduced gravity the experiment is mechanically decoupled with the RCM from the structure of the drag shield in five degrees of freedom. During microgravity time the experiment floats free inside the drag shield to achieve the highest possible microgravity quality.

The main advantage of novel drop towers is the higher repetition rate. During one hour of testing, the GraviTower Prototype performs 80 flights what equals to a mean repetition time of 45 s. The maximum repetition rate of the GraviTower Prototype is 960 flights per day and is effectively only limited by the turnover time of the experiments flown. Also, the system is capable to perform two subsequent flights. Furthermore the hydraulic accumulator of the drive could be extended if necessary for some experiments. To enable the highest possible repetition rates under campaign conditions the GraviTower Prototype offers automated supply of the experiment inside the slider between flights with power, data, media, cooling, and vacuum venting. Direct access to the experiment between flights for manual operations is also possible. It takes approximately 10 s after flight to lock the slider and open the doors to get full access. Furthermore, the

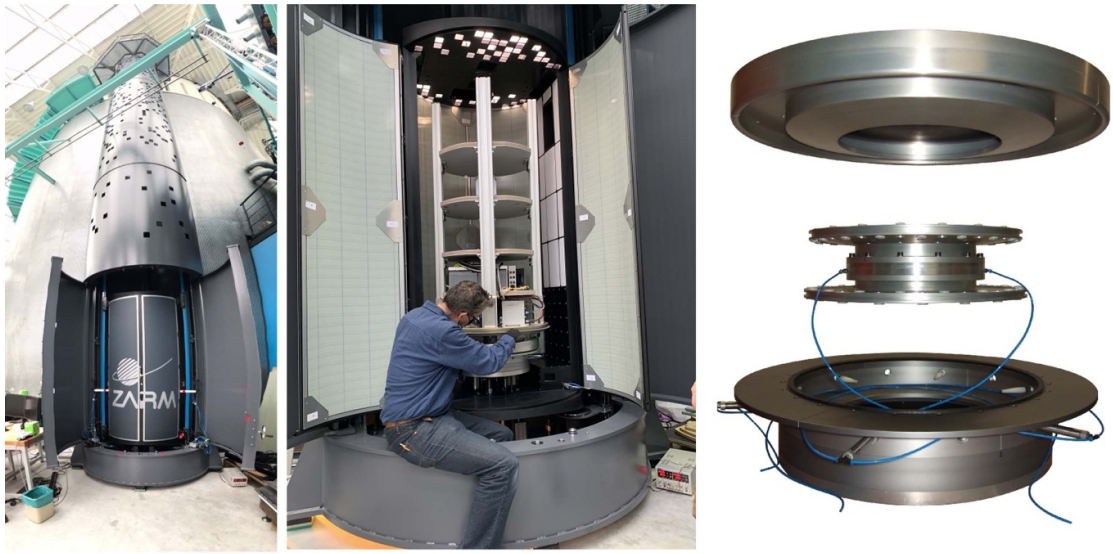

Figure 4. The GraviTower Prototype at ZARM, University Bremen, with open slider doors to access the payload and details of the Release-Caging-System.

experiment can be rotated inside the slider freely to get easy access to every part of the experiment. After closing the doors the GraviTower Prototype is immediately ready for the next flight. These features are implemented to achieve the highest possible repetition rates for a great variety of experiments.

The GraviTower Prototype is designed for the same payloads as the Bremen drop tower, discussed in section 3.2. The maximum payload size is 0.85 m^3 and up to 500 kg, offering full compatibility between the two facilities.

Therewith campaigns with a combined use of the GraviTower Prototype, drops and catapult shots in the Bremen drop tower with 9.3 s of microgravity, are possible.

Each experiment capsule comes equipped with a CCS (capsule computer system). As part of the included service by the drop tower Service Company (ZARM Fab) every experiment team is supported by at least two engineers for typically two weeks for the integration, automation and testing of the experiment in the ZARM experiment capsule before the campaign. The CCS can be used to automate the experiments and also to collect and downlink the data for the experiment. Next to the CCS a variety of high-speed cameras are available if useful. The CCS also offers live-view into the experiment at any time also during flight, continuous data downlink and communication between the ground control user interface of the experiment and with the GraviTower.

With a total height of 16 m, the GraviTower Prototype offers a microgravity duration of 2.5 s or any reduced gravity like Lunar gravity (2.8 s) or Martian gravity (3.4 s). Also changing gravity levels during one flight are possible like g-level sweeps. Due to the harmonic low frequency time function of the initial acceleration the full 2.5 s are usable microgravity time as no structural vibrations occur that have to decay first. The hydraulic rope drive offers a pre-tensioning of the ropes before flight to achieve a latency-free start. This allows the experiment to perform any kind of time critical pre-procedure before flight.

The quality of microgravity demonstrated in 2021 to be better than $10^{-4}\,g$ up to 50 Hz for full size experiments. Above 50 Hz acoustic forces from the slider walls act on the experiment. To improve the quality at higher frequencies acoustic absorbers are currently mounted inside the slider. For small experiments that fit on one single platform (like retro-reflector mirrors) an additional free-flyer system is designed to mechanically decouple that one platform from the structure of the experiment capsule. Residual accelerations below $10^{-6}\,g$ are realistically aimed at. The RCM is designed to not only decouple the experiment in five degrees of freedom during the initial acceleration but also during reduced gravity. As a further improvement an active RCM is in development, which will create the vertical force vector for partial gravity by a linear drive to allow a mechanical decoupling of the experiment also in the vertical translational degree of freedom.

All kinematic parameters of the GraviTower Prototype, like the amplitude of the initial acceleration, the micro- or decigravity level and the amplitude of the deceleration can be set by the users in a wide range. For full automation the GraviTower Prototype and the experiment can be linked together allowing the experiment to define the kinematic parameters of the flight, trigger the flight and to request supplies. A fully autonomous operation of the GraviTower Prototype together with the experiment is therewith possible. The settings of the GraviTower Prototype kinematics can be used as an extension of the experiments parameter

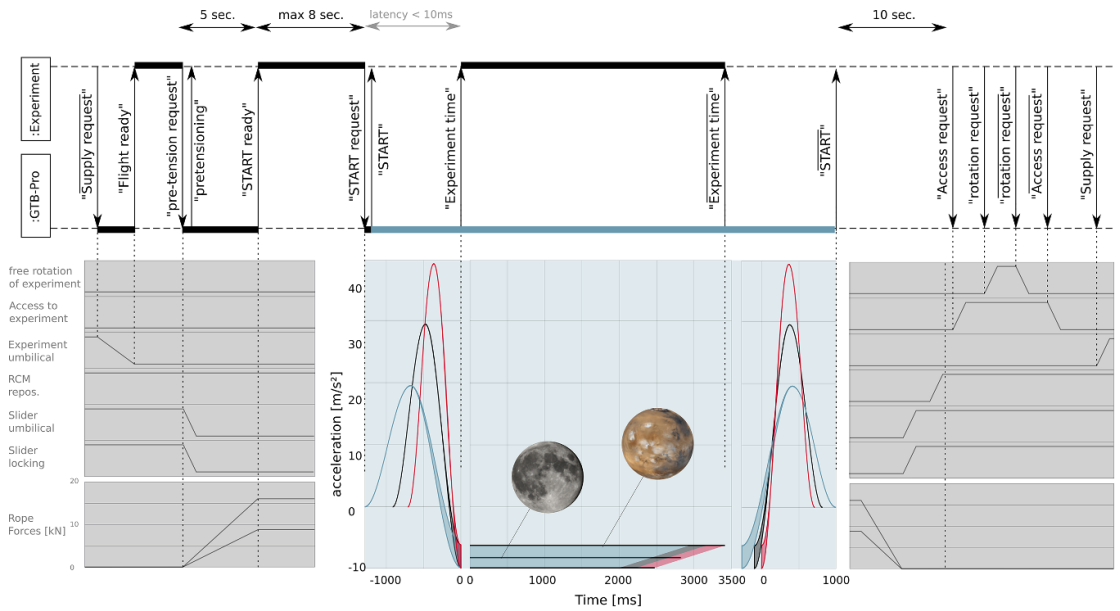

Figure 5. Details of one flight sequence of the GraviTower Prototype at ZARM, University Bremen. The communication between the experiment and the tower is visible on top and the possible kinematics are visible in the bottom center.

space for optimizations in the execution of the experiment. All data collected by the GraviTower Prototype (accelerations, pressures, forces and imperfections of any kind) is offered to the experiment and experimenters with highly accurate time stamps for use in automated and/or AI data analyses.

Figure 5 shows the kinematics of the GraviTower Prototype comparing three different amplitudes of initial acceleration, three different levels of gravity during the test time and also three different amplitudes for deceleration (bottom center). Left and right of the kinematics the possible pre- and post procedures including supplying the experiment and getting access to the experiment are shown. At the top of figure 5, a sequence diagram shows the communication between the GraviTower Prototype and the experiment. The maximum initial acceleration and deceleration is 4 g dynamic (5 g total) but can be lowered to 1 g dynamic for very acceleration sensitive experiments. The transition from the initial acceleration into the test acceleration can be smoothed by adding another cosine function to the acceleration time function (not shown in the figure). Next to weightlessness other partial gravity levels up to Martian gravity can be chosen.

The main drawback of this facility is the limited experiment time. However, the GraviTower Prototype allows a very high repetition rate combined with a fully adjustable kinematic. As the system is prepared for an autonomous operation, it is possible for experiments to operate the tower. Due to the easy access to the experiment between flights never before seen workflows become possible. Due to the medium size of the experiments every experiment developed and integrated for the GraviTower Prototype could also be operated on the Einstein-Elevator.

3.4. Parabolic flight

Parabolic flights employ airplanes to generate microgravity conditions. For this a maneuver of ascend followed by the ignition into a parabolic trajectory and a pull out into normal flight configuration is performed. The phases of the flight are depicted on the Novespace homepage [60]. The plane is first subjected to a 1.8 g hyper-g phase during which the airplane ascends. It is then injected into the parabola, lasting for 22 s. During this time the airplane falls freely in the gravitational potential leading to the experience of microgravity inside of the plane. Afterwards, the airplane is pulled out of the parabola before it is back in nominal flight configuration. During a flight usually 31 parabolas are flown.

Throughout the maneuver the plane is controlled by three pilots, to allow for smooth transitions, low roll, and a straight trajectory. With this control, microgravity stability is in the range of $\pm 0.02\,g$ [60]. From the start to the end of the parabola maneuver, the airplane rotates 92 degrees in negative pitch direction [60].

To achieve the calmest environment, the scientific experiments are mounted to the mid-section of the plane, where a total of 100 m^2 [60] of area is available. After completion of the flight, the full vibrational spectrum, as recorded by the plane, is handed to the researchers to compare to their experimental data. The total mass of the scientific instruments is 4000 kg [60]. Usually experiments are expected to have a mass around 100 kg and are required to state their center of mass. With that information, the experiments are

distributed inside the cabin. Large experiments, which take up the entire space are not unheard of and possible for the plane to accommodate.

A usual flight campaign lasts for two weeks. During the first week the researchers and their experiments arrive on site. They are given some time to prepare the experiments and load them into the plane. During this time, the safety instructions are provided to the researchers and human subjects. On three following days, daily flights are performed, after which the experiments are removed from the plane.

Parabolic flights, offer several advantages over the other ground-based facilities:

- The researchers can execute the experiments themselves and manipulate the system in real time.
- Human test subjects are possible, allowing to study a wide variety of subjects with high statistics.
- While the plane experiences 1.8 g of hypergravity, this is much less compared to the impact of, for example a sounding rocket launching and landing.
- The plane supplies power to the experiments during flight.
- Large and heavy experiment can be accommodated.

The main disadvantages of the parabolic flights are the high level of residual vibrations caused by the people on board, the air surrounding the plane, and the flight parameter. Other disadvantages are the rotation, the limited amount of flights available to researchers, especially with respect to active drop towers, and the additional safety regulations that have to be observed.

French researchers in the I.C.E collaboration have achieved atom optics experiments in a hybrid sensor on this platform such as light-pulse atom interferometry, atom-interferometric accelerometry with a sensitivity of $2 \cdot 10^{-4}\,\mathrm{ms}^2\,\mathrm{Hz}^{-1/2}$ and accelerations resolved 300 times below typical fluctuations onboard the aircraft. They tested the equivalence principle, measuring the Eötvös parameter with an uncertainty of $3 \cdot 10^{-4}$ [23, 61, 62].

3.5. Sounding rockets

Rockets to LEO use most of their propulsion capability Δv to reach orbital velocity—much more than to reach the orbit height potential

$$\Delta v = v_\mathrm{e} \ln \frac{m_0}{m_\mathrm{f}}.$$

Equation 2. Tsiolkovsky rocket equation where v_e is the exhaust velocity, m_0 is the initial rocket wet mass and m_f is the final mass of the rocket after propulsion. For multistage rockets, the equation must be computed for each stage separately.

According to the Tsiolkovsky rocket equation (equation (2)), the rocket wet mass scales exponentially with increased Δv requirements. Because of the high mass required for orbit, the size, energy and launch cost of orbiting rockets are high. Sounding rockets reach space altitudes, but do not accelerate to orbital velocities for orbital insertion. This dramatically decreases size, energy and launch cost per payload mass.

After launch, sounding rockets follow a steep parabolic trajectory. Then, the second stage burns out, separates and de-spin systems are activated to stabilize the payload. As the rocket leaves the atmosphere on a sub-orbital trajectory (free falling), the lack of atmospheric drag force creates the desired microgravity environment. At the end of the microgravity period, a mild atmospheric reentry happens with the help of heatshield and parachutes. The payload is then retrieved by helicopter with the help of a beacon.

The European Space and Sounding Rocket Range (ESRANGE) is next to Kiruna in northern Sweden, 150 km north of the polar circle. ESA has launched sounding rockets for over 30 years from this site. The remoteness of the site allows unguided launches with a large uninhabited recovery area of 5600 km^2 [64]. A unique feature of ESRANGE is its pyramid-shaped launch tower, as visible in figure 6. The tower allows launch preparations without the interference of the arctic climate. ESRANGE also features ground support facilities to monitor and control every aspect of the launch. The proximity to Kiruna allows relatively good accessibility with roads. Kiruna has a train connection to norway and central europe and an international airport.

'Mobile Raketenbasis' (ger. mobile rocket base—MORABA), is a department of DLR. They provide sounding rocket research platforms for atmospheric, hypersonic and microgravity research [65]. Parts of its portfolio consists of military surface-to-air motors, which are decommissioned and demilitarized, allowing a competitive price. The rockets range starts from the 'Improved Orion', visible in figure 7 on the left, which can carry light payloads up to ≈80 kg for short duration microgravity research [66]. The MAXUS and TEXUS rockets are based of the VSB-30 platform, which allows long duration microgravity with medium

Figure 6. MAPHEUS-7 launch from ESRANGE Space Center with visible launch tower (credit: DLR (CC BY-NC-ND 3.0), [63]). Reproduced with permission from [63].

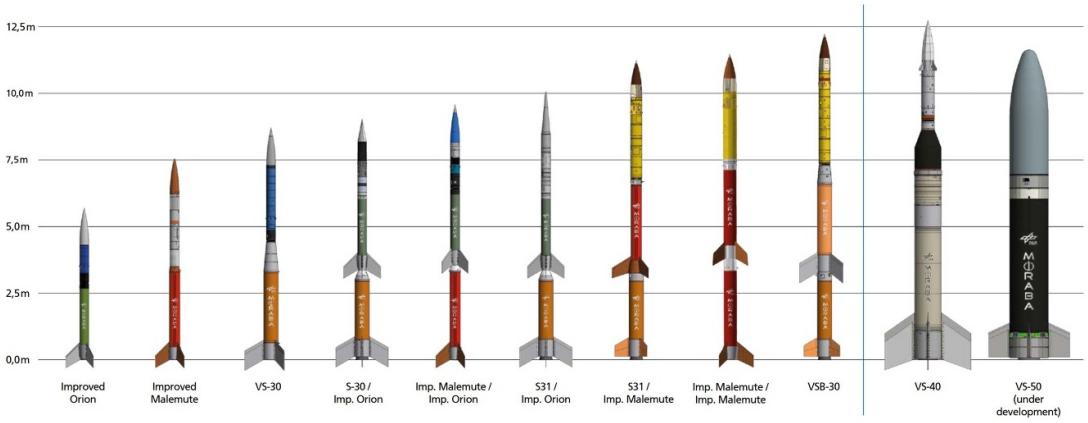

Figure 7. MORABA sounding rocket models, as taken from [65]. The two rockets VS-40 and VS-50 on the right are guided. Reproduced with permission from [65].

payloads. The achievable apogee (furthest point from Earth) depends on the available energy of the rocket motor, but mostly the ratio $\frac{m_0}{m_f}$ of the initial mass m_0, containing the fuel and the final mass m_f. (equation (2)) The final mass consists ideally only of the payload and recovery systems. Therefore, the reachable apogee for a rocket type is highly dependent on the payload mass. A graphical representation of that dependency can be found in [65, 66]. In table 1, the relevant example configurations are compared. Rockets with a high apogee, like the VS-40 and VS-50 would have a large impact area without active guidance, assuring not to exceed the ESRANGE area. For rockets with a smaller apogee, like the 'Improved Orion' until VSB-30, as visible in figure 7 on the left, a ballistic trajectory is sufficient. The duration of microgravity is the time the rocket spends above the atmosphere. Comparable with drop towers with catapult or active towers, half of the time above the atmosphere is spent ascending to the apogee and the other half descending to the edge of the atmosphere. On a suborbital steep parabolic trajectory, the total microgravity time is dependent on the reachable apogee [65].

The two stage MORABA large sounding rocket VS-50 is currently under development in Phase D. Due to the increase of propulsion capability, the rocket will reach payload masses of up to 1000 kg and altitudes of 2600 km, which equates to 1800 s (30 min) of microgravity [66, 68]. Sounding rockets offer one main advantage over the other ground-based facilities: The microgravity time of several minutes with a high stability of 10^{-5}–$10^{-6}\,g$ [65]. With this advantage, compromises have to be made with regards to mission

Table 1. Brief comparison of MORABA rocket models example configurations including TEXUS, MAXUS [67] and VSB-50 [66, 68] sounding rockets.

	TEXUS VSB-30	MAXUS Castor 4B	VSB-50
Payload diameter	438 mm	640 mm	1500 mm
Scientific payload mass	270 kg	500 kg	1000 kg
Apogee	250 km	750 km	2600 km
Free fall time	400 s	730 s	1800 s

design. The mission cost is comparably very high per launch. However, experiments can be recovered and reused. Furthermore, the full impact area at ESRANGE is only available during winter. Another constraint is the payload weight and size, limiting the microgravity time. During ascent and landing, the rocket endures high acoustics and accelerations of several g, which could damage the payload.

The MAIUS-1 Mission performed 110 experiments during the flight and achieved the creation of a BEC with 10^5 atoms in 1.6 s and BEC interferometry on this platform [44, 45].

4. Facility comparison

In table 2, the microgravity time, repetition rate and stability are summarized. Cold Atom Experiments favor a long free fall time and stability, for higher accuracy, precise measurements and higher sensitivity, as described in section 2. A high repetition rate allows more data runs, which lead to better statistics or an and extended parameter space. Furthermore, accessible facilities with high repetition rates allow debugging and changing parameters during an experimental run.

From this table it is visible, that all facilities have a unique performance envelope and therefore the choice of the microgravity facility depends strongly on the requirements for the experiments.

For instance, if a very long microgravity time is preferable over large statistics, the drop tower with catapult and sounding rockets are good options. The sounding rockets have by far the longest maximum microgravity time, but the actual flight time are however limited by the mass, as discussed in section 3.5. All drop towers operate or plan to achieve a microgravity stability better than 10^{-6} g. If repetition rates and accessibility are the dominant experiment requirements, active drop towers, like the Einstein-Elevator and the GraviTower Prototype are favoured.

In table 3, the operational payload constraints, as size and available flight masses are compared between the discussed facilities. Parabolic flights can accommodate large and heavy payloads, but this space is often shared with other experiments. These flights are the only facility allowing direct payload interaction during microgravity by the operator. The other experiments can accommodate payloads of comparable mass and size, which in principle allows designing an experiment for operation in different facilities. The GraviTower Prototype and the Bremen drop tower are specifically designed to be compatible and the Einstein-Elevator is even slightly less restrictive. This synergy enables combined campaigns, which take advantage of the best of the individual facilities, specifically high repetition rates and long microgravity times.

The novel drop towers offers features like the mentioned very high repetition rates and reduced gravity but also, depending on the facility, less obvious features that allow and necessitate new experimental workflows. Some of the new features will be summarized here for a brief discussion on the impact on the experimental workflows.

Besides reduced gravity, the Einstein-Elevator offers hyper-g with direct transition to μg, comparable to the stage separation during a rocket launch. This opens the parameter space for the experiments to a wide range of gravitational states. The GraviTower Prototype offers variable g-levels during one flight, including negative gravity, called g-vectoring. Different to the established conventional drop towers the experiments remain inside the sliders of the new drop towers between flights. The experiments can be supplied with electricity, cooling/heating and venting or other media upon need inside the slider. Also manual work on the experiments, like changing samples, is possible inside the sliders. Active drop towers are prepared to be partly controlled by the experiment itself. This includes requesting supply between flights and triggering the flight sequence. In return, the towers communicate their status to the experiment. Furthermore, the experiments can adjust the kinematics to their needs automatically. The new drop towers offer variable latency between the expected time of transition into microgravity to the real beginning of microgravity as low as 10 ms. Precise timed preparations of the experiment before the flight get possible. Also, as the new towers are fully active, very low initial accelerations of below 1 g dynamic and below 2 g total acceleration are possible. Smoother time functions of this initial acceleration and transitions into microgravity also become possible. This may mitigate the drawback of comparatively short microgravity durations.

Table 2. Comparison of μg facilities.

Facility	Free fall time	Repetition rate	Stability better than
Einstein-Elevator	4 s	300 per day	$10^{-6}\,g$
Drop tower	4.7 s	3 per day	$10^{-6}\,g$
Drop tower with catapult	9.3 s	3 per day	$10^{-6}\,g$
GraviTower Prototype	2.5 s	960 per day	$10^{-4}\,g$
Parabolic flight	20 s	31 parab. per flight	$2 \cdot 10^{-2}\,g$
Sounding rockets	up to 13 min	single flight	$10^{-5}\,g$

Table 3. Comparison of payload constraints of μg facilities.

Facility	Payload Size	Mass
Einstein-Elevator	d = 1.7 m, h = 2.0 m	1000 kg
Drop tower	d = 0.6 m, h = 1.7 m	500 kg
Drop tower with catapult	d = 0.6 m, h = 0.95 m	400 kg
GraviTower Prototype	d = 0.6 m, h = 0.95 m	500 kg
Parabolic flight	avail. area = 100 m^2	4000 kg
Sounding rockets	d = 0.64 m	up to 800 kg

4.1. Desired future platforms

Rapid development has taken place in recent years, particularly in the case of drop towers. This development is not yet complete, as large active systems are being planned at ZARM in Bremen and at NASA in Cleveland. For this reason, the most important potentially possible features of these future systems are discussed as briefly as possible in the following.

A critical parameter previously discussed is the repetition rate. Active drop towers make several hundred flights per day possible. With some modifications more than a thousand flights per day become possible in existing and also in larger future facilities.

According to equation (1), microgravity durations of around 10 s, as in the Bremen drop tower with catapult, require a minimum vertical falling distance of 122.6 m. Due to the quadratic function, increasing the falling distance leads to a minor microgravity time increase. Also, forces on the mechanism and the payload are higher by the increasing velocities. Therefore, the 10 s fall time range is plausible in new, active drop towers.

Between flights, it is very useful to access the experiment. This allows semi-automated experiments and changes to the experiment during the campaign. In active towers, this can be possible with low turnover times. Therewith even not fully automated experiments can make use of high repetition rates.

For cold atom experiments, the stability of microgravity is also an important factor. The novel drop towers still have to demonstrate a microgravity quality of $10^{-6}\,g$. If even better stabilities are of scientific interest the planned larger facilities could include more complex damping and additional free-flyer-systems. To improve microgravity and rotation stability besides the vertical translational degree of freedom, micro- and millinewton thrusters on the experiment can be used to control turn rates. The targeted precision is turning rates below 1 mrad/s defined on all three axis.

In drop towers, some experiments can be influenced by the magnetic field from the supporting steel structure. Future drop towers could be built avoiding ferromagnetic materials in the building and in the guiding system. The sliders of the new drop towers can be designed to include Helmholtz coils, compensating the terrestrial magnetic field or setting a desired magnetic field. Big Helmholtz coils in the slider offer a bigger and smoother magnetic field than smaller H-Coils inside the payload.

Bigger experiments are more comfortable to integrate. Increasing the level of integration and miniaturization is time and cost intensive. However, the weight also plays a major role in the tower design. Smaller experiment structures on the other hand are stiffer and therewith more suitable for higher microgravity stability. Empirical values from the Einstein-Elevator and the GraviTower Prototype can help to find the most suitable experiment design for future drop towers.

On the ISS, complex experimental setups usually are build and carried out in so called 'express racks'. These are standardized steel framework containers with a size of a refrigerator (height: 2 m, width: 1.05 m, depth: 85.9 cm). Until now, the experiments are prepared and lab tested before their flight to the ISS. In the future, active drop towers, as the Einstein-Elevator, open the possibility to embark complete express racks. With this a perfect copy of a space payload can be tested regarding the science capabilities for 4 s on Earth. This is a great opportunity to demonstrate the maturity of critical designs and complex concepts. Technical

demonstrations before leaving Earth could also become an additional key to get funding for a mission by space agencies.

Other operational factors not mentioned in the table 3 are the automation and timing of the experiments. As previously mentioned in section 4, active drop towers are already capable to be operated by the experiment itself and automatically adjust the kinematics. This is possible by adjusting parameters like the amplitude of the initial acceleration, the transition into microgravity and the amplitude of the deceleration. A smooth transition into microgravity leads to less parasitic vibrations during the precious microgravity time, allowing earlier and better data points.

The new drop towers require precise timing. A small latency of the transition time into microgravity allows precise preparations of the experiment before flights.

Between flights, the experiment can be connected to power, cooling, a data connection or media like vacuum can be exchanged automatically. A Lab-Information-Management-Systems (LIMS), as commonly used in ground-based labs, should be implemented as the high repetition rates necessitate such systems. LIMS includes support for the experimental data handling. It allows automised high speed connections to external high performance clusters for the evaluation of the data. Furthermore it supplies the experiments with all the available recorded data from the towers. This can enable future AI algorithms to evaluate and adapt the experiment data in real-time.

Future drop towers can include safety infrastructure like radiation and laser protection as parts of the drop tower. This allows scientists to prepare critical experiments safely in a laboratory environment directly inside the sliders of the drop towers. Secondary safety features like safe storage places, uninterruptible power supply (UPS) and exhaust treatments are advantages that only drop towers can provide compared to other microgravity platforms.

From the point of view of the experimenter, the main difference with the new facilities is the change in how campaigns are carried out. So far campaigns are prepared and carried out while the collected data is analysed. As the new facilities offer more flights and the possibility to work on the experiment between flights, operation can be closer to standard lab practices. This includes direct evaluation of the collected data after each flight and more complex campaign planning and preparation, considering and making use of the new possible outcomes of the first flights.

5. Cold atom experiments in ground-based microgravity platforms

5.1. Ground-based verification of orbital platforms and pathfinder experiments

There is a number of mission proposals for orbital platforms conducting cold atom experiments ranging from fundamental physics [27, 29] to applications like gravity field mapping [28, 32, 69–72]. A risk for these experiments is that the involved techniques have only barely or never been tested in the absence of gravity. Therefore, these methods have a low technological readiness level and present a considerable risk for the success of future space missions on orbital platforms. Models of ground-based experiments consider known effects, either from literature or the experiment itself, including specific technical details. These models may be incomplete when extrapolating to a space-borne setup. Interferometry with freely falling atoms was tested up to a total duration of 2.3 s [73] while proposals for space-borne sensors target 10 s and more [31, 69, 74, 75]. Atom interferometric techniques involving symmetric matter-wave beam splitters and mirrors [76, 77], higher-order diffraction or large momentum-transfer [78] are mostly being used in experiments on ground under influence of gravity. For quantum tests of the equivalence principle, the behaviour of atom mixtures trapped under microgravity conditions can be vastly different compared to conventional setups. Due to the absence of the differential gravitational sag, an increased thermalization rate during sympathetic cooling close to the phase transition is expected [79]. Also, the ground state of trapped interacting mixtures in microgravity can lead to new states which cannot be observed under influence of gravity [80]. Techniques for massively reducing the momentum spread of expanding cold ensembles to achieve ultralong expansion times require new and untested protocols for atom mixtures [81, 82].

The possibility of the GraviTower Prototype and the Einstein-Elevator to probe different acceleration levels between terrestrial gravity and microgravity is very appealing in this context since it can be used to better understand the influence of gravity on the performance of these instruments or methods.

Furthermore, a number of proposals for future space missions [74, 75, 83] involve atom interferometers based on a clock transition and employing the same elements as state-of-the-art optical atomic clocks, such as Sr or Yb. This kind of interferometers can find applications in searches of ultralight dark matter [84], gravitational-wave detection [85, 86] and tests of the universality of free fall (UFF) with atoms in a quantum superposition of internal states [87, 88]. However, in contrast to alkali metals such as Rb, the TRL for future experiments with Sr or Yb atoms in space is still rather low. Therefore, pathfinder experiments with Sr or Yb on ground-based microgravity platforms would be very valuable for future space missions [74, 75, 89].

Moreover, the associated technological development would greatly benefit not only spaceborne atom interferometry experiments based on a clock transition, but also the prospects for having highly stable optical atomic clocks in space, which will have remarkable applications in metrology, geodesy and fundamental physics [33, 34].

5.2. Atom interferometry for fundamental physics measurements

5.2.1. Test of the equivalence principle

The UFF is a central aspect of Einstein's equivalence principle, which constitutes a cornerstone of the theory of general relativity. Differential acceleration measurements between two different atomic species and relying on atom interferometry [29, 90, 91] have experienced a remarkable progress in recent years, where ground tests of UFF have improved by 5 orders of magnitude in about half a decade [19] and are closely approaching the best sensitivities attained with macroscopic masses.

Since the interferometric phase shift caused by the acceleration increases quadratically with the interferometer time, a considerable sensitivity enhancement is enabled by longer free evolution times, which can be achieved with compact set-ups in microgravity platforms. However, unwanted effects associated with rotations and gravity gradients will also grow with longer interferometer times, leading to loss of contrast and challenging systematic effects that result in very demanding requirements on the initial co-location of the atomic clouds of the two species [92–94].

A technique for mitigating the effects of gravity gradients through a suitable frequency change of the laser pulses [95] has been implemented in recent experiments and proven to be very effective [19, 96]. Moreover, in space missions it can be combined with orbital modulation methods for further suppression of such effects [97]. Similarly, the effects of rotations can be compensated by means of a tip-tilt mirror for the retro-reflection of the laser beams [92]. In this way, the effects of Earth's rotation in atom interferometry can be successfully compensated [73, 98]. However, this relies on the fact that Earth's angular velocity is very stable. In contrast, for certain ground-based microgravity platforms the stability from shot to shot may be significantly lower as far as rotations are concerned [23].

Compared to other facilities such as 10 m atomic fountains, atom interferometry experiments on ground-based microgravity platforms can naturally enable a better co-location of the two atomic species, especially when employing different chemical elements rather than just different isotopes [81]. On the other hand, achieving the required rotation stability from shot to shot as well as the required magnetic shielding may be challenging.

5.2.2. Dark energy

Some dark-energy models involve very light scalar fields with a significant coupling to matter density. Such light fields would mediate long-range interactions resulting in a 'fifth' force that would lead to violations of UFF in stark contradiction with current experimental bounds on such violations. Chameleon and symmetron fields [99, 100] can circumvent this limitation because in the presence of matter densities much higher than the cosmological average (such as the Earth density or even the density of atmospheric air) they acquire a large effective mass that results in short-range interactions and the screening of macroscopic source masses except for a thin outer layer.

Atoms in a vacuum chamber are not affected by this screening mechanism and are therefore particularly well-suited test masses for sensing forces mediated by chameleon and symmetron fields [101–103]. Furthermore, atom interferometers can be sensitive to the small accelerations caused by such forces. Thus, ground-based experiments with atom interferometers have substantially improved the bounds on such models [104–106]. However, freely falling atoms can only spend a short time close enough to a macroscopic mass within the vacuum chamber that acts as a source for the scalar fields. In contrast, microgravity environments enable long interferometer times during which the freely evolving atoms can remain close to the source mass, which results in a substantial increase in sensitivity [50].

By combining the use of suitable spatially periodic mass sources and atom interferometers with multiloop geometries, one can achieve large sensitivities to the effects of chameleon and symmetron fields while mitigating the effects of rotations and gravity gradients [50, 107]. Indeed, atom interferometers involving an even number of loops suppress the main contribution of rotations and when combined with a suitable frequency change of the intermediate pulses [95], gravity gradients can also be compensated.

5.3. Shell-shaped quantum gases

In the absence of residual gravitational forces undisturbed potentials allow for new topologies for quantum gases in microgravity which offer unique properties and an experimental playground to investigate quantum gases in reduced dimensions.

For example, driving a topological transition from filled three-dimensional ensembles to hollow two-dimensional shells would enable to study quantum gases in two-dimensional curved geometries embedded in three-dimensional space. Furthermore, the topology is predicted to have influence on vortex dynamics, few-body physics and molecule formation [108–110]. However, the experimental realization of quantum bubbles has been hindered yet by the presence of gravity.

As initially proposed by Zobay and Garraway [111, 112], inhomogeneous magnetic fields can be overlapped with an rf field to generate adiabatic potentials to trap neutral atoms. In case of an Ioffe–Pritchard like magnetic trap, this leads to spherical, two-dimensional shell potential in which atoms can be trapped and which has been demonstrated by various experiments [113, 114]. Without gravity compensation techniques, the formation of uniformely filled shells is not possible. Although optical potentials have been proposed to mitigate the influence of gravity [112], the implementation of such a scheme has not been demonstrated yet. Due to the experimental difficulties in evenly compensating gravity, the ideal setting to create shell-shaped adiabatic potentials is naturally given by a microgravity environment. This approach is now followed by the Cold Atom Laboratory which demonstrated the successful generation of shell potentials on-board the International Space Station [37, 38].

An alternative way to generate shell-shaped quantum gases is to employ a dual-species mixture with inter-species repulsion generated in an optical diople trap in absence of gravity. This naturally leads to a radial phase separation between the two gases resulting in a two-dimensional shell of the outer component [80]. The generation of interaction driven condensate shells does not rely on rf adiabatic potentials but solely on the condensation of two interacting gases in a common trap. This scheme could be realized in future experiments with a device like BECCAL, but is also conceivable for state-of-the-art two-species experiments in ground-based microgravity facilities. Promising initial results using this scheme have been recently been obtained in a sodium-rubidium mixture configuration [115].

Another technique to generate shell BECs is given by outcoupling of atoms from a magnetic trap by low-intensity rf fields, also known as the atom laser [116]. In the absence of gravity, the outcoupling mechanism becomes spatially symmetric which leads to a spherical expanding shell condensate [117]. The experimental generation of BEC shells is now in its early stages of development and numerous experiments are conceivable in the future. Microgravity facilities like the Einstein-Elevator or drop towers represent ideal facilities to perform such experiments.

6. Conclusion

For more than 20 years cold atom experiments have been performed in drop towers. Many great scientific feats like the first BEC in microgravity, the first matter-wave interferometry with such BECs and a high-flux source of BEC were achieved. Besides these scientific achievements, technology developments on the experiments were carried out which now enable the BECCAL mission on the International Space Station. Cold atom research benefits strongly from microgravity environments due to the negative influence of the gravitational sag on the atoms. In atom interferometry for example, long evolution times lead to to more precise measurements due to an increase in the separation of the interferometer arms. Current and emerging scientific opportunities for cold atom research and the corresponding experiments have been discussed.

With direct accessibility for the researchers, the ground-based facilities are a useful solution for performing experiments under microgravity, testing hypothesis and developing technologies. Several different ground-based microgravity facilities are discussed in this article. With these facilities both fundamental research and technology development can be executed, creating not only an important bridge between laboratory and space-based experiments, but also excel in scientific research by themselves. As the experimental and technological requirements are different, a comprehensive comparison between the facilities has been provided. Apart from the main factors, like free-fall time and repetition rate, payload-centric factors, programmatic limitations and operational aspects have to be considered as well. All the discussed facilities are less expensive and more easily accessible than space missions, while each working with a different set of unique features. Already from the comparison it can be concluded, that the leader of an experiment has to carefully consider their requirements and then choose the appropriate facility.

Regardless of the individual choice or preference, all of the mentioned operational facilities are well booked, demonstrating the necessity for the accessibility of microgravity environments. With that note, the authors want to encourage further next-generation facilities and therefore defined future platform parameters. Such platforms will allow easier access and higher repetition rates for more experiments and future advancements.

Data availability statement

All data that support the findings of this study are included within the article (and any supplementary files).

ORCID iDs

Matthias Raudonis https://orcid.org/0000-0002-2858-8112
Albert Roura https://orcid.org/0000-0002-8049-8982
Matthias Meister https://orcid.org/0000-0001-7210-8588
Christoph Lotz https://orcid.org/0000-0003-0324-8274
Ludger Overmeyer https://orcid.org/0000-0002-7734-8895
Sven Herrmann https://orcid.org/0000-0001-8195-580X
Claus Lämmerzahl https://orcid.org/0000-0002-8276-5415
Nicholas P Bigelow https://orcid.org/0000-0003-1854-5757
Maike Lachmann https://orcid.org/0000-0003-4212-0863
Baptist Piest https://orcid.org/0000-0003-0488-4504
Naceur Gaaloul https://orcid.org/0000-0001-8233-5848
Waldemar Herr https://orcid.org/0000-0002-3685-2729
Christian Deppner https://orcid.org/0000-0002-1911-4433
Wolfgang Ertmer https://orcid.org/0000-0001-7912-5495
Nathan Lundblad https://orcid.org/0000-0003-0430-8064
Lisa Wörner https://orcid.org/0000-0002-8808-5891

References

[1] Clement G B R and Gunga H-C 2019 *Front. Physiol.* **10** 1447
[2] Grosse J *et al* 2012 *FASEB J.* **26** 639–55
[3] Aubry-Hivet D *et al* 2014 *Plant Biol.* **16** 129–41
[4] Steinberg T A, Wilson D B and Benz F 1992 *Combust. Flame* **88** 309–20
[5] Nishikawa K, Fukunaka Y, Chassaing E and Rosso M 2013 *Electrochim. Acta* **100** 342–9
[6] Mathiak G, Plescher E and Willnecker R 2005 *Meas. Sci. Technol.* **16** 336
[7] Eigenbrod C, Klinkov K, Peters M, Marks G, Paa W, Wagner V and Triebel W 2016 *Int. J. Microgr. Sci. Appl.* **33** 330306
[8] Thoma M H, Höfner H, Kretschmer M, Ratynskaia S, Morfill G E, Usachev A, Zobnin A, Petrov O and Fortov V 2006 *Microgr. Sci. Technol.* **18** 47
[9] van Zoest T *et al* 2010 *Science* **328** 1540–3
[10] Grond J, Hohenester U, Mazets I and Schmiedmayer J 2010 Atom interferometry with trapped Bose–Einstein condensates: impact of atom–atom interactions (available at: https://doi.org/10.1088/1367-2630/12/6/065036)
[11] Moes M J, Gielen J C, Bleichrodt R J, van Loon J J W A, Christianen P C M and Boonstra J 2011 *Microgr. Sci. Technol.* **23** 249–61
[12] Rothermel H, Hagl T, Morfill G E, Thoma M H and Thomas H M 2002 *Phys. Rev. Lett.* **89** 175001
[13] Urban D 2015 Modification plans for the nasa 5.2 second drop tower *Annual Meeting of the American Society for Gravitational and Space Research* (GRC-E-DAA-TN28101)
[14] 2021 Nasa glenn 2.2 second drop tower (available at: www1.grc.nasa.gov/facilities/drop/)
[15] 2021 Kingston micro-gravity drop tower (available at: www.ukspacefacilities.stfc.ac.uk/Pages/Kingston-Micro-Gravity-Drop-Tower.aspx)
[16] Liu T, Wu Q, Sun B and Han F 2016 *Sci. Rep.* **6** 1–9
[17] 2021 Hokkaido univeristy jamic mg facility (available at: http://lsu-eng-hokudai.main.jp/en/facility/)
[18] Hartwig J, Abend S, Schubert C, Schlippert D, Ahlers H, Posso-Trujillo K, Gaaloul N, Ertmer W and Rasel E M 2015 *New J. Phys.* **17** 035011
[19] Asenbaum P, Overstreet C, Kim M, Curti J and Kasevich M A 2020 *Phys. Rev. Lett.* **125** 191101
[20] Abe M *et al* 2021 *Quantum Sci. Technol.* **6** 044003
[21] Zhou L *et al* 2015 *Phys. Rev. Lett.* **115** 1–5
[22] Frye K *et al* 2021 *EPJ Quantum Technol.* **8** 1
[23] Barrett B, Antoni-Micollier L, Chichet L, Battelier B, Lévèque T, Landragin A and Bouyer P 2016 *Nat. Commun.* **7** 13786
[24] Leanhardt A E, Pasquini T A, Saba M, Schirotzek A, Shin Y, Kielpinski D, Pritchard D E and Ketterle W 2003 *Science* **301** 1513–5
[25] Deppner C *et al* 2021 *Phys. Rev. Lett.* **127** 100401
[26] Müntinga H *et al* 2013 *Phys. Rev. Lett.* **110** 093602
[27] Aguilera D *et al* 2014 *Class. Quantum Grav.* **31** 115010
[28] Zahzam N *et al* 2022 *Remote Sens.* **14** 3273
[29] Bassi A *et al* 2022 arXiv:2211.15412
[30] Williams J, Chiow S w, Yu N and Müller H 2016 *New J. Phys.* **18** 025018
[31] Battelier B *et al* 2021 *Exp. Astron.* **51** 1695–736
[32] Lévèque T *et al* 2021 *J. Geod.* **95** 1–19
[33] Müller J and Wu H 2020 *J. Geod.* **94** 71
[34] Müller J, Dirkx D, Kopeikin S M, Lion G, Panet I, Petit G and Visser P 2018 *Space Sci. Rev.* **214** 1–31
[35] Bertoldi A *et al* 2021 *Exp. Astron.* **51** 1417–26
[36] Alonso I *et al* 2022 arXiv:2201.07789
[37] Lundblad N, Carollo R A, Lannert C, Gold M J, Jiang X, Paseltiner D, Sergay N and Aveline D C 2019 *npj Microgr.* **5** 30

[38] Carollo R A, Aveline D C, Rhyno B, Vishveshwara S, Lannert C, Murphree J D, Elliott E R, Williams J R, Thompson R J and Lundblad N 2022 *Nature* **606** 281–6
[39] Pasquini T A, Saba M, Jo G B, Shin Y, Ketterle W, Pritchard D E, Savas T A and Mulders N 2006 *Phys. Rev. Lett.* **97** 093201
[40] Navarro R, Carretero-González R and Kevrekidis P G 2009 *Phys. Rev.* A **80** 023613
[41] Roth R and Burnett K 2004 *Phys. Rev.* A **69** 021601
[42] Varoquaux G, Nyman R A, Geiger R, Cheinet P, Landragin A and Bouyer P 2009 How to estimate the differential acceleration in a two-species atom interferometer to test the equivalence principle (https://doi.org/10.1088/1367-2630/11/11/113010)
[43] Woltmann M, Vogt C, Herrmann S and Lämmerzahl C 2022 *Bull. Am. Phys. Soc.* E04.002
[44] Becker D *et al* 2018 *Nature* **562** 391–5
[45] Lachmann M D *et al* 2021 *Nat. Commun.* **12** 1317
[46] Rudolph J, Herr W, Grzeschik C, Sternke T, Grote A, Popp M, Becker D, Müntinga H, Ahlers H and Peters A 2015 *New J. Phys.* **17** 065001
[47] Lotz C, Froböse T, Wanner A, Overmeyer L and Ertmer W 2017 *Gravitat. Space Res.* **5** 11–27
[48] 2021 Desire (available at: www.iqo.uni-hannover.de/en/research-groups/quantum-sensing/research-projects/search-for-dark-energy/)
[49] Chiow S W, Yu N, Roura A, Lachmann M D, Rasel E and Schkolnik V 2021 *Atomic Dark Energy Detection in space—Topical Whitepaper for BPS Decadal Survey 2021* (available at: http://surveygizmoresponseuploads.s3.amazonaws.com/fileuploads/623127/6378869/154-dcf482baa8379cbc38c2d9d1308371b6_ChiowShengwey.pdf)
[50] Chiow S W and Yu N 2018 *Phys. Rev.* D **97** 044043
[51] Lotz C, Gerdes N, Sperling R, Lazar S, Linke S, Neumann J, Stoll E, Ertmer W and Overmeyer L 2020 *Logistics J.: Proc.* **2020** 12
[52] Reitz B *et al* 2021 *Microgr. Sci. Technol.* **33** 25
[53] Moonrise 2021 (available at: www.lzh.de/en/publications/pressreleases/2021/moonrise-step-by-step-towards-a-village-made-of-moon-dust)
[54] 2021 Staubiges plasma (available at: www.uni-giessen.de/ueber-uns/pressestelle/pm/135-21staubigesplasmaineinsteinsaufzug)
[55] Lotz C, Wessarges Y, Hermsdorf J, Ertmer W and Overmeyer L 2018 *Adv. Space Res.* **61** 1967–74
[56] Lotz C 2022 Studies on influences to quality of experiments under microgravity in the Einstein-Elevator *PhD Thesis* Leibniz Universität Hannover
[57] Touboul P *et al* 2017 *Phys. Rev. Lett.* **119** 231101
[58] Watanabe S I, Tsuda Y, Yoshikawa M, Tanaka S, Saiki T and Nakazawa S 2017 *Space Sci. Rev.* **208** 3–16
[59] Rudolph J 2016 Matter-wave optics with Bose-Einstein condensates in microgravity *Dissertation* Leibniz Universität Hannover
[60] Novespace 2021 Air Zero G (available at: www.airzerog.com/)
[61] Stern G *et al* 2009 *Eur. Phys. J.* D **53** 353–7
[62] Geiger R *et al* 2011 *Nat. Commun.* **2** 474
[63] DLR 2023 Liftoff der forschungsrakete mapheus (Accessed 25 October 2022) (available at: www.dlr.de/de/bilder/institute/materialphysik-im-weltraum/mapheus)
[64] DLR 2007 Texus—research in weightlessness, misson brochure (Accessed 22 October 2021) (available at: https://moraba.de/en/downloads-specials/)
[65] DLR 2022 Moraba—portfolio sounding rocket flight experiments (Accessed 25 June 2022) (available at: www.dlr.de/rb/en/desktopdefault.aspx/tabid-17499/)
[66] DLR 2020 Moraba—sounding rocket launch vehicles (Accessed 25 October 2021) (available at: https://moraba.de/en/downloads-specials/)
[67] Schütte A and Grothe D 2005 Sounding rocket program: minitexus, texus and maxus *17th ESA Symp. on European Rocket and Balloon Programmes and Related Research* vol 590 pp 481–5
[68] DLR 2021 Successful static firing test with dlr involvement (Accessed 25 October 2021) (available at: www.dlr.de/content/en/articles/news/2021/04/20211007_s50-rocket-motor-for-microlaunchers.html)
[69] Carraz O, Siemes C, Massotti L, Haagmans R and Silvestrin P 2014 *Microgr. Sci. Technol.* **26** 139
[70] Trimeche A *et al* 2019 *Class. Quantum Grav.* **36** 215004
[71] Chiow S W, Williams J and Yu N 2015 *Phys. Rev.* A **92** 063613
[72] Knabe A, Schilling M, Wu H, HosseiniArani A, Müller J, Beaufils Q and Pereira dos Santos F 2022 *Int. Association of Geodesy Symposia*
[73] Dickerson S M, Hogan J M, Sugarbaker A, Johnson D M S and Kasevich M A 2013 *Phys. Rev. Lett.* **111** 083001
[74] El-Neaj Y A et al 2020 *EPJ Quantum Technol.* **7** 6
[75] Hogan J M and Kasevich M A 2016 *Phys. Rev.* A **94** 033632
[76] Lévèque T, Gauguet A, Michaud F, Pereira Dos Santos F and Landragin A 2009 *Phys. Rev. Lett.* **103** 080405
[77] Ahlers H *et al* 2016 *Phys. Rev. Lett.* **116** 173601
[78] Gebbe M *et al* 2021 *Nat. Commun.* **12** 2544
[79] Piest B 2021 Bose-Einstein condensation of K-41 and Rb-87 on an atom chip for sounding rocket missions *PhD Thesis* Leibniz Universität Hannover
[80] Wolf A, Boegel P, Meister M, Balaž A, Gaaloul N and Efremov M A 2022 *Phys. Rev.* A **106** 013309
[81] Corgier R, Loriani S, Ahlers H, Posso-Trujillo K, Schubert C, Rasel E M, Charron E and Gaaloul N 2020 *New J. Phys.* **22** 123008
[82] Meister M and Roura A 2022 arXiv:2207.07045
[83] Tino G M *et al* 2019 *Eur. Phys. J.* D **73** 228
[84] Arvanitaki A, Graham P W, Hogan J M, Rajendran S and Van Tilburg K 2018 *Phys. Rev.* D **97** 075020
[85] Graham P W, Hogan J M, Kasevich M A and Rajendran S 2013 *Phys. Rev. Lett.* **110** 171102
[86] Yu N and Tinto M 2011 *Gen. Relativ. Gravit.* **43** 1943–52
[87] Rosi G, D'Amico G, Cacciapuoti L, Sorrentino F, Prevedelli M, Zych M, Brukner C and Tino G M 2017 *Nat. Commun.* **8** 15529
[88] Roura A 2020 *Phys. Rev.* X **10** 021014
[89] Loriani S *et al* 2019 *New J. Phys.* **21** 063030
[90] Fray S, Diez C A, Hänsch T W and Weitz M 2004 *Phys. Rev. Lett.* **93** 240404
[91] Schlippert D, Hartwig J, Albers H, Richardson L L, Schubert C, Roura A, Schleich W P, Ertmer W and Rasel E M 2014 *Phys. Rev. Lett.* **112** 203002
[92] Hogan J M, Johnson D M S and Kasevich M A 2008 arXiv:0806.3261
[93] Roura A, Zeller W and Schleich W P 2014 *New J. Phys.* **16** 123012

[94] Kleinert S, Kajari E, Roura A and Schleich W P 2015 *Phys. Rep.* **605** 1–50
[95] Roura A 2017 *Phys. Rev. Lett.* **118** 160401
[96] Overstreet C, Asenbaum P, Kovachy T, Notermans R, Hogan J M and Kasevich M A 2018 *Phys. Rev. Lett.* **120** 183604
[97] Loriani S, Schubert C, Schlippert D, Ertmer W, Pereira Dos Santos F, Rasel E M, Gaaloul N and Wolf P 2020 *Phys. Rev.* D **102** 124043
[98] Lan S Y, Kuan P C, Estey B, Haslinger P and Müller H 2012 *Phys. Rev. Lett.* **108** 090402
[99] Khoury J and Weltman A 2004 *Phys. Rev.* D **69** 044026
[100] Hinterbichler K and Khoury J 2010 *Phys. Rev. Lett.* **104** 231301
[101] Burrage C, Copeland E J and Hinds E A 2015 *J. Cosmol. Astropart. Phys.* JCAP03(2015)042
[102] Elder B, Khoury J, Haslinger P, Jaffe M, Müller H and Hamilton P 2016 *Phys. Rev.* D **94** 044051
[103] Chiow S W and Yu N 2020 *Phys. Rev.* D **101** 083501
[104] Hamilton P, Jaffe M, Haslinger P, Simmons Q, Müller H and Khoury J 2015 *Science* **349** 849–51
[105] Jaffe M, Haslinger P, Xu V, Hamilton P, Upadhye A, Elder B, Khoury J and Müller H 2017 *Nat. Phys.* **13** 938–42
[106] Sabulsky D O, Dutta I, Hinds E A, Elder B, Burrage C and Copeland E J 2019 *Phys. Rev. Lett.* **123** 061102
[107] Ufrecht C, Roura A and Schleich W P 2021 arXiv:2107.03709
[108] Sun K, Padavić K, Yang F, Vishveshwara S and Lannert C 2018 *Phys. Rev.* A **98** 013609
[109] Tononi A, Cinti F and Salasnich L 2020 *Phys. Rev. Lett.* **125** 010402
[110] Bereta S J, Caracanhas M A and Fetter A L 2021 *Phys. Rev.* A **103** 053306
[111] Zobay O and Garraway B M 2001 *Phys. Rev. Lett.* **86** 1195–8
[112] Zobay O and Garraway B M 2004 *Phys. Rev.* A **69** 023605
[113] Colombe Y, Knyazchyan E, Morizot O, Mercier B, Lorent V and Perrin H 2004 *Europhys. Lett.* **67** 593–9
[114] Hofferberth S, Lesanovsky I, Fischer B, Verdu J and Schmiedmayer J 2006 *Nat. Phys.* **2** 710–6
[115] Jia F, Huang Z, Qiu L, Zhou R, Yan Y and Wang D 2022 Expansion dynamics of a shell-shaped bose-einstein condensate *Phys. Rev. Lett.* **129** 243402
[116] Robins N, Altin P, Debs J and Close J 2013 *Phys. Rep.* **529** 265–96
[117] Meister M, Roura A, Rasel E M and Schleich W P 2019 *New J. Phys.* **21** 013039